Field effect in InAs/permalloy hybrid transistors

G. Meier, T. Matsuyama, and U. Merkt
Universität Hamburg, Institut für Angewandte Physik und Zentrum für Mikrostrukturforschung, Jungiusstraße 11, D-20355 Hamburg, Germany

(Received 9 April 2001; revised manuscript received 25 October 2001; published 13 March 2002)

We measure the static and dynamic resistance of metal-oxide-semiconductor field-effect transistors with ferromagnetic source and drain contacts deposited on InAs at liquid helium and elevated temperatures. The field effect is examined as a function of the applied gate voltage in external magnetic fields applied in plane either parallel or perpendicular to the current direction. In the parallel configuration the resistance exhibits strong evidence for spin-polarized transport via an oscillatory gate-voltage dependence of the resistance jumps at the irreversible magnetization reversals of the ferromagnetic electrodes. Furthermore, transport measurements in external magnetic fields aligned perpendicular to the substrate surface are performed up to strengths of 14 T to investigate the properties of the semiconductor channel, i.e., charge-carrier concentration, electron mobility, and weak localization.

DOI: 10.1103/PhysRevB.65.125327 PACS number(s): 72.25.−b, 73.23.Ad, 71.70.Ej, 73.61.Ey

I. INTRODUCTION

The investigation of the possible role of electron spin in solid-state devices on semiconductors is a highly attractive and vivid field of research because of both basic physical questions and technological aspects.[1] An important step in this direction was the proposal of Datta and Das in 1990 to build an analogue to the electro-optical modulator for electron spins in a low-dimensional electron system of a semiconductor,[2] which nowadays is addressed as spin field-effect transistor. In their proposal Datta and Das envisaged a ballistic device incorporating a one-dimensional electron channel in a semiconductor that admits of a tunable Rashba effect. Two ferromagnetic electrodes exhibiting 100% spin polarization with fixed collinear magnetizations serve as injector and detector of spin-polarized electrons in their device. In principle, all basic components inevitable for the preparation of such a spin transistor are now available. One important prerequisite is the possibility to control spin polarization via spin-orbit interaction in form of the Rashba effect. Two-dimensional electron systems (2DES's) on InAs are promising candidates to satisfy this condition because they possess a strong spin-orbit interaction originating from two basic contributions, which are due to bulk inversion asymmetry and structure inversion asymmetry, respectively.[3,4] While the first contribution is owing to the zinc-blende structure of the crystal itself the latter consists of two parts, which can be tuned at will. The latter two are caused by the strong electric field perpendicular to the plane of the 2DES and the asymmetric penetration of the electron wave function into the barriers confining the 2DES, respectively. In heterostructures the second part is found to be the dominating one,[5] while in single-crystal samples with inversion layers at their surfaces the electric-field contribution plays the important role.[6] The Rashba effect lifts the spin degeneracy of the energy dispersion[7] and generates a spin precession by an angle $\theta = 2m^*\alpha L/\hbar^2$ with the effective electron mass m^*, the channel length L, and the Rashba parameter α. Because of its importance for a possible realization of a spin transistor several groups have investigated the gate-voltage dependence of the strength of the spin-orbit coupling and thus of the Rashba parameter for quantum wells in heterostructures[4,5,8,9] as well as for inversion layers on bulk InAs.[6] A marked gate-voltage dependence is found in both systems.

The control of the spin state would be of no relevance if spin coherence could not be guaranteed in the channel. With the help of optical detection several experiments have proved convincingly[10,11] that this condition is easily fulfilled for GaAs. Due to the stronger spin-orbit interaction in InAs the electron-spin coherence time is smaller in comparison with GaAs,[12] but still large enough for the realization of a ballistic device with a channel length in the sub-μm range. Besides control and coherence of the spin states a sufficient number of spin-polarized charge carriers has to be provided by a source electrode.[2] One approach for injection and detection of defined spin states are ferromagnetic electrodes.[13] Due to exchange coupling they can provide a surplus of one type of charge carriers, say, spin-up or spin-down electrons at the Fermi energy. A perfect electrode material would provide 100% spin polarization at the Fermi energy as can be expected from Heusler alloys.[14,15] For materials like Fe and permalloy, that are presently employed, the efficiency of spin injection is comparatively low but recent experiments have shown that injection of spin-polarized carriers is feasible.[16,17] A recent optical experiment has proven that a spin-polarized current can be injected from a Fe layer into a GaAs quantum well through a Schottky barrier with a spin-injection efficiency of 2%.[18]

Here, we describe experiments on the electron transport in metal-oxide field-effect transistors (MOSFET's) on bulk InAs with ferromagnetic permalloy electrodes that are magnetized by external magnetic fields applied along or perpendicular to the current direction. We focus on the gate-voltage dependence of the channel resistance, i.e., on the field effect, which yields clear signatures of spin-valve and spin-precession effects. We discuss our experimental findings within the framework of a model for spin-polarized ballistic transport. This model accounts for the finite width of our contacts by incorporating oblique modes as it is adequate for 2DES's. Although we are confident that the interpretation of

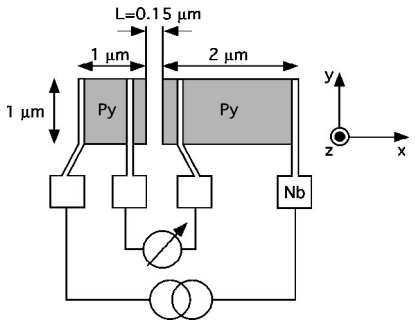

FIG. 1. Geometry of the permalloy ($Ni_{80}Fe_{20}$) source and drain contacts as well as of the superconducting Nb probes that enable definite four-terminal measurements.

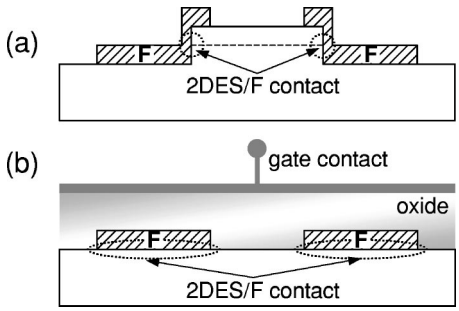

FIG. 2. Sketch of the surface geometries for (a) heterostructures and (b) bulk crystals. While the etched surface of heterostructures provides a complicated three-dimensional situation for the magnetic domain structure, for the single-crystal devices the semiconductor surface and the ferromagnetic contacts are flat. The dotted circles in (a) and ellipses in (b) indicate the linear and planar contact area, respectively.

the data in the framework of this model is correct we like to note already at this point that in principle an alternative explanation in terms of weak localization/antilocalization may exist. Detailed analyses and control measurements of the gate-voltage, the temperature, and the magnetic-field dependence of the weak localization effects suggest that they are rather unlikely to explain the observed phenomena.

II. PREPARATION

In this investigation we employ permalloy ($Ni_{80}Fe_{20}$) source and drain contacts on *p*-type InAs (100) single crystals, which exhibit native 2DES at their surfaces. Permalloy is used as electrode material since it possesses a considerable degree of spin polarization of approximately 40% at the Fermi energy[14] and no magnetostriction effects due to the compensation of the Ni and the Fe contribution. The 18-nm-thick permalloy contacts with a protective cap layer of 9 nm Au were deposited by thermal evaporation at a pressure of 10^{-8} mbar. Energy dispersive x-ray analysis (EDX) of the electrode structures confirmed the composition of 80% Ni and 20% Fe. A four-terminal setup of 100-nm-thick Nb leads patterned by electron-beam lithography was deposited by dc magnetron sputtering[19] and optically defined wiring is used for electrical contacts. Superconducting Nb leads allow us definite and precise four-terminal measurements despite the native inversion layer that resides all over the InAs surface. The metal-oxide semiconductor field-effect transistor (MOSFET) is completed by a gate oxide (350 nm) grown by plasma enhanced chemical vapor deposition (PECVD) and a gate contact consisting of 40 nm Al and 10 nm Au both thermally evaporated. Figure 1 shows a sketch of the source- and drain-contact geometry. The voltage probes on top of the permalloy contacts are prepared in close proximity to the channel. This virtually eliminates resistance effects which might occur in the metallic contacts themselves, e.g., the anisotropic magnetoresistance (AMR). The asymmetric ferromagnetic contacts permit switching of the magnetization at definite external magnetic-field strengths.[13,20] This is essential to obtain defined magnetization configurations in the magnetic domains next to the channel.

As argued in the introduction, InAs is the semiconductor of choice because of its strong and tunable spin-orbit interaction. In particular, we choose *p*-type InAs single crystals, on which native inversion layers establish 2DES's at their surfaces under the gate oxide. InAs forms Ohmic contacts to virtually all metals, i.e., there is no Schottky barrier as found in most GaAs/metal contacts. Thus the resistance of the contact itself is small compared to a diodelike contact which is the case for GaAs. An important advantage, especially in comparison with heterostructures, is the contact shape. In heterostructures the contact between ferromagnetic metal and 2DES is a narrow area located at the side of the etched mesa structure as depicted in Fig. 2(a). It is only a few nanometers wide. Due to the etching process the quality of the ferromagnet/2DES interface is difficult to control. For inversion layers on InAs single crystals the situation is more advantageous in this respect as sketched in Fig. 2(b). Here, the contact geometry is flat and the contact area is large. The quality of the contact is much easier to control since physical and chemical polishing and an optional *in situ* rf cleaning process directly prior to the deposition of the ferromagnetic metal are feasible.[19] A disadvantage of the planar device is its less well defined channel length. Provided their sheet resistances become comparable, the source and drain contacts and the 2DES underneath them compete for the current flow towards the channel. In our device, however, the ratio of the sheet resistances gives rise to a quasiedge injection of the current. On the other hand, the planar geometry and the simple shape of its ferromagnetic contacts guarantee a micromagnetic behavior which is well understood[21] and can be simulated[22,23] and measured.[13] Thus the magnetic behavior can be well controlled when *p*-type InAs single crystals are employed as substrates.

III. EXPERIMENTAL RESULTS

In the absence of a magnetic field, the source-drain resistance as a function of the gate voltage is depicted in Fig. 3. From these data a specific contact resistance between ferromagnet and 2DES of 10^{-7} $\Omega\,\mathrm{cm}^2$ is estimated indicating a high contact quality. The observed $R(V_g)$ curve is typical for MOSFET's. In the depicted regime above the threshold voltage $V_g=-17$ V the resistance decreases with increasing gate voltage V_g and concomitantly increasing carrier concen-

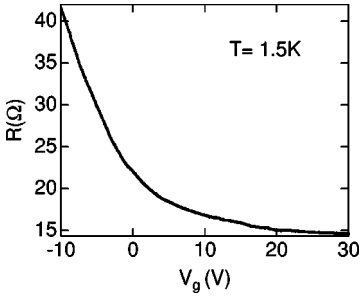

FIG. 3. Total resistance versus gate voltage at $T=1.5$ K.

tration n_s.[24] Due to surface roughness scattering at the oxide/semiconductor interface[25,26] the electron mobility decreases from about 20 000 $\mathrm{cm^2\,V^{-1}\,s^{-1}}$ at low gate voltages monotonically to about 9000 $\mathrm{cm^2\,V^{-1}\,s^{-1}}$ at higher ones. Accordingly, we evaluate mean free paths of about 230–100 nm which are comparable to the nominal channel length of our device, which is the edge to edge spacing between the source and drain electrode. Thus we can tune the electron mean free path from the quasiballistic to the diffusive regime. We emphasize that both mobility and carrier concentration are strictly monotonic functions of the gate voltage in the range of gate voltages examined here. In order to determine the dependence of the electron density and the Rashba parameter on the gate voltage, an analysis of Shubnikov–de Haas oscillations was performed. Strong magnetic fields ($B \leqslant 14$ T) were applied perpendicular to the surface of the present sample as well as to similar samples on the same wafer.[6] Period in $1/B$ and beating pattern of the oscillations yield electron density and Rashba parameter, respectively.[4–6,8,9] From the Rashba parameter[6] we calculate for the nominal channel length of $L=150$ nm a maximum change of the spin precession angle $\Delta\theta=1.1\ \pi$ at the highest voltage $V_g=+30$ V. Thus, one expects one-half of an oscillation in the spin-controlled resistance according to the model of Datta and Das.[2] At this point we would like to mention that in their model the oscillations are expected for charge carriers which exhibit 100% spin polarization and are injected with their spins aligned in the x-z plane (see Fig. 1). Only for this alignment the electrons occupy a mixed state with respect to the Rashba Hamiltonian and the spin itself becomes involved in the interference process. In other words, an oscillatory resistance is expected only if there is a component of the magnetization in the electrode that is parallel to the current direction. This situation, in which the magnetic field is applied along the x direction, is addressed as spin-transistor configuration in the following. When the magnetization is perpendicular to the current direction the electrons are injected into an eigenstate with respect to the Rashba Hamiltonian and therefore the spin inside the semiconductor is conserved. This situation with the magnetic field applied along the y direction we call the spin-valve configuration. No oscillatory resistance effects are expected then. In the experiments the two configurations are realized via the direction of the externally applied magnetic field and the resulting alignment of the magnetizations in the ferromagnetic electrodes.

Before we describe the measurements in the spin-valve and spin-transistor geometry we first turn to experiments that

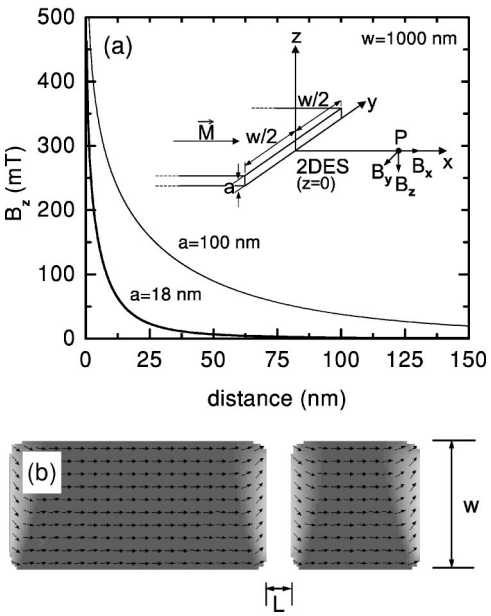

FIG. 4. (a) Calculated stray-field component B_z for the magnetization of a permalloy electrode at point P with a saturation magnetization of $M_S=800$ kA/m. (b) Micromagnetic simulation of a permalloy electrode pair of the experimental device geometry $L=150$ nm and $w=1\ \mu$m at $B_x=+40$ mT. Right next to the channel the magnetic moments and the x axis enclose an angle of approximately 45° in this example.

we have performed to investigate a possible influence of other magnetoresistance effects. Most important, we carefully examined a possible role of fringe-field effects[27,28] caused by the magnetization of the permalloy electrodes. In the inset of Fig. 4(a) the principal geometry of our device with the 2DES and the ferromagnetic thin film lying in essentially the same plane, which is the surface of the InAs crystal, is visualized. Because of symmetry reasons the perpendicular component of the magnetic stray field B_z virtually vanishes. On the other hand, ignoring extremely weak diamagnetic shifts of the electric subbands,[29] the 2DES is only influenced by perpendicular magnetic fields. The data in Fig. 4(a) present calculated strengths of the perpendicular field component B_z for two thicknesses a of the permalloy electrodes.[30] An angle of 45° between the x axis and the direction of the magnetization vector is set for the calculation. This is a reasonable assumption in externally applied magnetic fields in the mT regime along the x direction as shown in Fig. 4(b). The values of the field component B_z become virtually independent of the channel width when it exceeds the film thickness ($w \gg a$). In fact, for our film thicknesses of $a=18$ nm the effective field B_z is virtually zero over most of the channel length L. Only right next to the contacts the field strength does not vanish. It amounts to 80 mT in a distance of 10 nm from a contact. This result is supported by μ-Hall magnetometry of ferromagnetic structures of the geometry used in this work.[31]

To further support that fringe fields cannot play a significant role in our devices complementary experiments in external perpendicular magnetic fields have been carried out to mimic the effect of fringe fields and to examine, in particular,

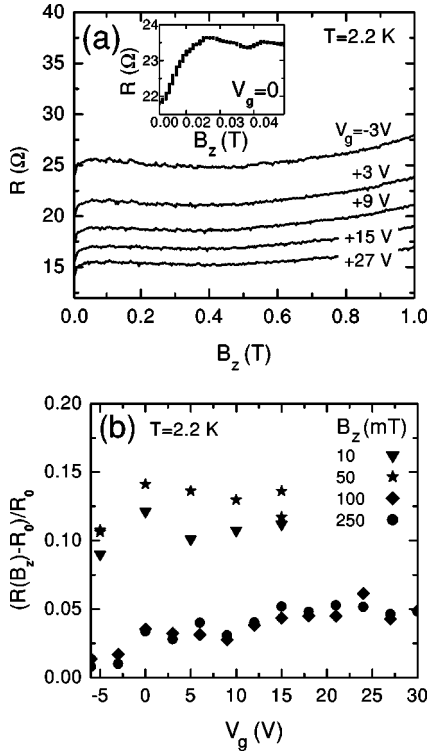

FIG. 5. (a) Source-drain resistance for various gate voltages versus strength B_z of an external magnetic field applied perpendicular to the plane of the 2DES. The inset shows a blow-up of the low-field data at zero gate voltage. The steplike structures are due to resolution limitations of the magnetic field sweep. (b) The normalized resistance difference is evaluated for various field strengths in order to mimic the influence of the switching magnetization.

a possible role of quantum corrections to the conductance due to weak localization.[32] Figures 5(a) and 5(b) show the result of this investigation. In the relevant range of magnetic field strengths of up to 250 mT, that in the presence of stray fields are realized only very close to the ferromagnetic source-drain contacts, the difference $R(B_z)-R_0$ is virtually constant in the whole regime of gate voltages. Hence weak localization cannot explain oscillatory resistance effects. Another contribution could be the AMR effect of the permalloy electrodes which, however, is independent of the gate voltage and hence should definitely be absent in gate-modulated measurements.

We now proceed to describe our experiments in spin-valve and spin-transistor geometry, respectively. The expected resistance changes due to spin-polarized transport with ferromagnetic electrodes not exhibiting 100% spin polarization are small[33–35] and we cannot expect their direct observation on the $R(V_g)$ curve. To make these effects visible we measure the resistance of the device at a fixed gate voltage when the magnetization of one of the electrodes is switched with respect to the other. The latter becomes possible as a consequence of their geometrical asymmetry[13,20] that is evidenced in Fig. 1.

We first discuss the results for the spin-valve experiments. In Fig. 6(a) the source-drain resistance is plotted versus the strength of the magnetic field when it is applied along the y direction. In the downsweep as well as in the upsweep of the magnetic field irreversible jumps in the resistance are clearly observed. We focus on these resistance jumps and attribute them to irreversible magnetization changes of the magnetic electrodes. The smooth background behavior of the resistance is presumably due to the reversible part of the magnetization change. The amplitude of the resistance jump at $+23$ mT is shown in the inset of Fig. 6(a). Within the error bar indicated there is no significant gate-voltage dependence.

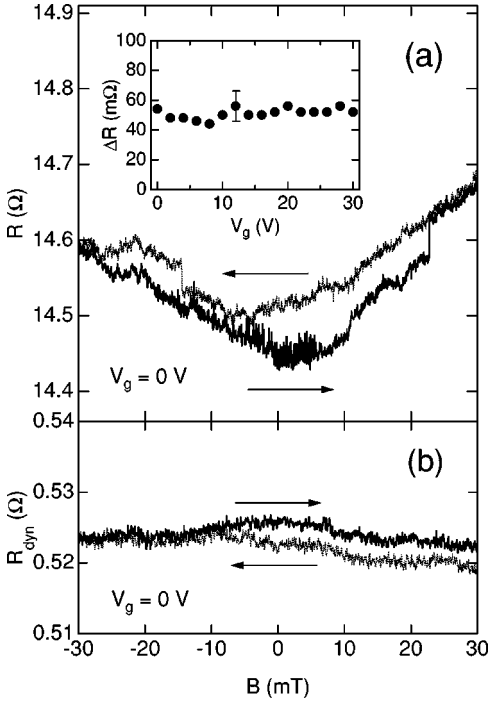

FIG. 6. Typical raw data of (a) the total and (b) the dynamical resistance recorded simultaneously at $T=1.5$ K. The magnetic field is applied perpendicular to the current direction ($B\|y$). The inset shows the amplitude of the irreversible jump in the total resistance at 23 mT.

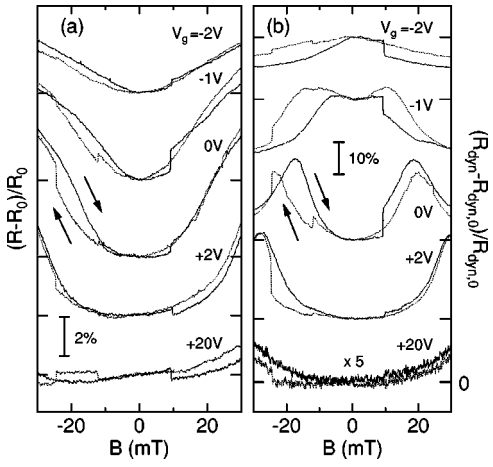

FIG. 7. Normalized (a) total and (b) dynamical resistance curves at $T=1.5$ K. The magnetic field is applied parallel to the current direction ($B\|x$). The traces are successively offset for clarity with the respective zeros indicated.

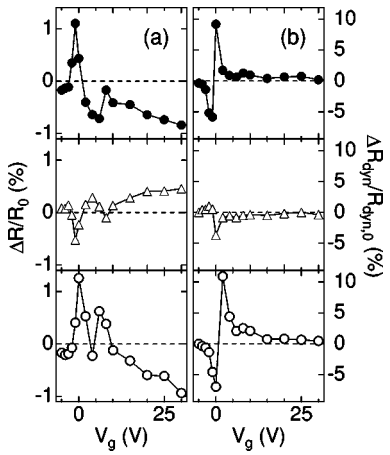

FIG. 8. Amplitudes of the normalized irreversible changes of (a) the total normalized source-drain resistance $\Delta R/R_0$ and (b) the dynamical resistance $\Delta R_{dyn}/R_{dyn,0}$. Filled circles denote jumps at $+9.0$ mT in upsweeps, open triangles and open circles jumps in downsweeps at -12.0 and -24.4 mT, respectively. The errors are comparable to the symbol sizes.

This is expected for this geometry where the spin state of the injected charge carriers represents an eigenstate with respect to the Rashba Hamiltonian. Interestingly, in the dynamical response R_{dyn} reproduced in Fig. 6(b) no irreversible resistance changes are observed. As this signal is measured by a lock-in technique with respect to the gate voltage ($f = 333$ Hz, $\Delta V_g = 0.5$ V) it should most directly display the response of the 2DES. AMR effects do not show up in this signal because AMR does not respond to a gate voltage. Weak localization effects, which exhibit a rather constant behavior with respect to the gate voltage (see Fig. 5), should consequently be rather small in the dynamical resistance. As discussed in the next section, the resistance in the spin-valve configuration is in fact not expected to be sensitive to electron density thus explaining the results of Figs. 6(a) and 6(b).

The situation is totally different for the spin-transistor configuration with the external magnetic field applied along the current direction ($B \| x$). Again, we observe distinct jumps in the normalized total resistance $(R-R_0)/R_0$ with zero-field resistance R_0. They are evident in Fig. 7(a). A surprising feature is a gate-controlled change of their signs, e.g., seen when the traces for gate voltages 0 and $+2$ V are compared. Strikingly, unlike in the perpendicular case, the normalized dynamic resistance $(R_{dyn}-R_{dyn,0})/R_{dyn,0}$ now exhibits irreversible jumps too. Both, the simultaneously measured irreversible jumps in the total and in the dynamical resistance are located at the same field values that correspond to irreversible magnetization changes of the permalloy electrodes.[13,20] As can already be seen directly from the raw data in Fig. 7(b) there is a significant gate-voltage dependence of the jump amplitudes. In the gate-voltage regime around $V_g = 0$ the amplitude is clearly larger than at higher and lower gate voltages. In Figs. 8(a) and (b) the normalized amplitudes $\Delta R/R_0$ and $\Delta R_{dyn}/R_{dyn,0}$ of the jumps are plotted versus gate voltage. More or less pronounced, they all show oscillatory behavior. The signals are most distinct at lower voltages and clearly weaker at higher ones.

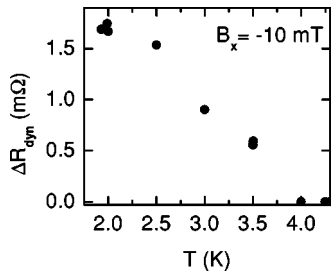

FIG. 9. Typical temperature dependence of a jump amplitude.

To conclude with the experimental data a typical temperature dependence of the jump amplitude is shown in Fig. 9. While fringe field Hall effects persist up to temperatures well above 100 K,[27] the jump amplitude vanishes already at about 4 K. This rapid decrease may be caused by a corresponding decrease of the spin coherence length, which is affected in the quasiballistic regime by spin-orbit coupling and thus by momentum scattering. The temperature dependence of the weak localization effects in Figs. 5 has been measured on the same device and differs from that for the jump amplitude in Fig. 9 inasmuch as weak localization survives up to temperatures of at least 9 K and shows a different curvature as a function of temperature.

IV. DISCUSSION

In this section we interpret our experimental results as spin injection and detection as well as modulation of the spin precession by a gate voltage. First, theoretical expectations for transport experiments with switching magnetizations in the ballistic regime are discussed. We compare the model of Datta and Das with an extended model taking into account a truly 2DES with oblique modes, ferromagnetic electrodes exhibiting restrained spin polarization, and spin filtering due to band-structure mismatch at the surfaces.[33–35,37]

In the pioneering work of Datta and Das the conductance G is expected to exhibit oscillations as a function of the strength of the Rashba effect, i.e., as a function of the gate voltage. Already from the simple ansatz $G \propto \cos^2(\theta/2)$ for the conductance[2] a sign reversal of ΔG can be expected at the hysteretic magnetization changes. There, the direction between spin polarization and magnetization is changed by a phase π and the resulting conductance jump can alter its sign according to the difference $\Delta G \propto \cos^2(\theta/2) - \cos^2[(\theta+\pi)/2] = \cos\theta$.

In principle, the above description is only valid for the strictly one-dimensional case but more recent theoretical work[36] has demonstrated that the essential features predicted by Datta and Das[2] survive for finite channel widths. In fact, in the real case one has to bear in mind the boundary conditions at the ferromagnet/semiconductor interface for majority and minority spin subbands and the two-dimensional nature of the electron system.[37] In a ballistic Landauer-Büttiker model,[33,34,38] we take both into account and calculate the dependence of the conductance on the carrier density for spin-valve and spin-transistor configuration in the two-dimensional case.[37] Figure 10(a) and (b) shows for both configurations the calculated conductance for parallel and anti-

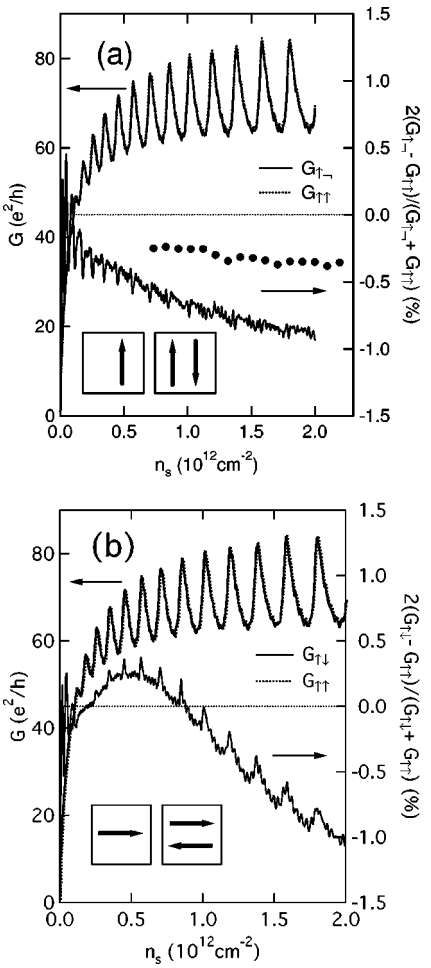

FIG. 10. (a) Calculated conductance for the spin-valve configuration in the parallel $G_{\uparrow\uparrow}$ (dotted line) and in the antiparallel $G_{\uparrow\downarrow}$ (light solid line) situation for channel length $L=150$ nm, channel width $w=1$ μm, and permalloy parameters (Ref. 39). The range of carrier concentration from 0.7×10^{12} to 2.0×10^{12} cm^{-2} corresponds to a gate voltage regime of 0–26 V. Also plotted is the normalized conductance difference $2(G_{\uparrow\uparrow}-G_{\uparrow\downarrow})/(G_{\uparrow\uparrow}+G_{\uparrow\downarrow})$. (b) Results for the spin-transistor configuration. The course of the conductance difference represents the original result of Datta and Das (Ref. 2) when averaged over the individual modes. Full circles are experimental data.

parallel alignment as well as the corresponding conductance difference $2(G_{\uparrow\uparrow}-G_{\uparrow\downarrow})/(G_{\uparrow\uparrow}+G_{\uparrow\downarrow})$ versus the carrier concentration. The large oscillations in the conductances are due to Fabry-Pérot interferences not treated by Datta and Das. They occur as a consequence of the two closely spaced ferromagnet/semiconductor interfaces. The tiny structures in the conductance differences result from the distinct number of modes that are summed up in our two-dimensional model.

The conductance difference for the spin-transistor configuration is totally different and sign changes are calculated as a function of the electron density as can be seen in Fig. 10(b). Thus the main features of the one-dimensional model of Datta and Das[2] persist in the two-dimensional situation. At first glance, this is astonishing as in the two-dimensional case also oblique modes with respect to the x direction contribute to the current. However, spin precession can only be obtained when the injected electron is a superposition of spin-up and spin-down eigenstates. In case of tilted injection the transmission coefficients as well as the directions of the momentum vectors of the spin-up and the spin-down eigenstates are no longer equal. Hence a mixed state, which produces significant spin interference due to the Rashba effect, cannot efficiently be injected into the 2DES. Furthermore, in the present devices a small angle selection is ensured by the ratio of coherence length and channel length which is not far from unity in the relevant gate-voltage regime. Therefore the effective channel length for electrons injected under a more significant angle with respect to the x axis becomes longer than the spin-coherence length and its contribution to the ballistic current becomes correspondingly less.

In the framework of the above theoretical description we now turn to the analysis of the experimental data of Figs. 6 and 7. As discussed in Sec. III reproducible and discrete changes of the total and the dynamical resistances R and R_{dyn} occur at the switching fields in both configurations. The result of the measurement in the spin-valve configuration ($B\|y$) is shown in the inset of Fig. 6(a). The resistance changes versus the gate voltage are virtually constant and especially exhibit no change of sign. The data of the inset of Fig. 6(a) normalized with the resistance of Fig. 3 can directly be compared to the theoretical result in Fig. 10(a). In the relevant density regime well above inversion threshold ($n_s \geqslant 0.7\times10^{12}$ cm^{-2}) the theoretical and the experimental data are in good correspondence and virtually unaffected by the gate voltage. Both exhibit no change of sign. The reduced amplitude of the experimental data could be attributed to real materials and interfaces which could not be accounted for in the model.

In the spin transistor configuration ($B\|x$) we consider the amplitudes of the dynamical resistances in Fig. 8(b) as these should most directly display the response of the 2DES itself. Based on the phase shift $\Delta\theta\cong1.1$ π that has been estimated above, we expect the conductance difference $\Delta G\propto\cos\theta$ to run through just one maximum and minimum in the entire interval $-5\leqslant V_g\leqslant+30$ V. In this regime we observe at least one full oscillation for two of the resistance changes in Fig. 8(b). An important feature in comparison to the result of Fig. 10(b) is that both experimental and theoretical data exhibit sign changes of conductance and resistance. However, the quantitative agreement is rather poor, e.g., the observed period of the oscillation is too short. At present we can nothing but speculate that the transition to the diffusive regime reduces the jump amplitude at higher gate voltages to zero and thus pretends a full oscillation in Fig. 8(b). Also, the current distribution between the permalloy films and the inversion layer in the InAs underneath them may elongate the nominal channel length and thus act in the same direction.

As mentioned in the introduction, in principle an alternative explanation in terms of modulation of weak localization and antilocalization due to magnetic stray fields may exist. But the distinct temperature dependence of the jump amplitude (see Fig. 9) and the weak localization supports the above interpretation. While we cannot rule out weak local-

ization effects in fringe fields, the experimental data hint at a minor role of them for the resistance jumps at the irreversible magnetization changes.

V. CONCLUSION

To conclude, we have observed oscillatory changes in the resistance of MOSFET's with ferromagnetic contacts in the spin-transistor geometry, i.e., when the external magnetic field is applied along the current direction. From a careful examination of the temperature- and gate-voltage dependence of the observed phenomena we deduce a minor role of possible parasitic effects in magnetic stray fields. In particular, we considered in detail AMR, local Hall effects, and weak localization. In the spin-valve geometry with the field applied perpendicular to the current we measure no gate-voltage dependence of the resistance changes. In accordance with the picture of precessing spins due to the Rashba effect, the oscillatory behavior only appears when the magnetization of the contacts points in the current direction. Also, the temperature dependence of the oscillations provides evidence that we may have achieved in principle the spin-transistor action envisaged ten years ago by Datta and Das.[2]

ACKNOWLEDGMENTS

We would like to thank D. Grundler, C.-M. Hu, and P. Středa for valuable discussions. The evaporation of the permalloy electrodes and their EDX analysis have been performed superbly by W. Pfützner. This work is supported by the Deutsche Forschungsgemeinschaft via the Sonderforschungsbereich 508 ''Quantenmaterialien'' and the NEDO International Joint Research Program.

[1] G.A. Prinz, Phys. Today **48**(4), 58 (1995).
[2] S. Datta and B. Das, Appl. Phys. Lett. **56**, 665 (1990).
[3] E.A. de Andrada e Silva, G.C. La Rocca, and F. Bassani, Phys. Rev. B **50**, 8523 (1994); **55**, 16 293 (1997).
[4] G. Engels, J. Lange, Th. Schäpers, and H. Lüth, Phys. Rev. B **55**, 1958 (1997).
[5] D. Grundler, Phys. Rev. Lett. **84**, 6074 (2000).
[6] T. Matsuyama, R. Kürsten, C. Meissner, and U. Merkt, Phys. Rev. B **61**, 15 588 (2000).
[7] R.H. Silsbee, Phys. Rev. B **63**, 155305 (2001).
[8] J.P. Heida, B.J. van Wees, J.J. Kuipers, T.M. Klapwijk, and G. Borghs, Phys. Rev. B **57**, 11 911 (1998).
[9] J. Nitta, T. Akazaki, H. Takayanagi, and T. Enoki, Phys. Rev. Lett. **78**, 1335 (1997).
[10] D. Hägele, M. Oestreich, W.W. Rühle, N. Nestle, and K. Eberl, Appl. Phys. Lett. **73**, 1580 (1998).
[11] D.D. Awschalom and J. Kikkawa, Phys. Today **52**(6), 33 (1999).
[12] W.H. Lau, J.T. Olesberg, and M.E. Flatté, Phys. Rev. B **64**, 161301 (2001).
[13] G. Meier and T. Matsuyama, Appl. Phys. Lett. **76**, 1315 (2000).
[14] R.J. Soulen, J.M. Byers, M.S. Osofsky, B. Nadgorny, T. Ambrose, S.F. Cheng, P.R. Broussard, C.T. Tanaka, J. Nowak, J.S. Moodera, A. Barry, and J.M.D. Coey, Science **282**, 85 (1998).
[15] R.A. de Groot, F.M. Mueller, P.G. van Engen, and K.H.J. Buschow, Phys. Rev. Lett. **50**, 2024 (1983); W.E. Pickett and J.S. Moodera, Phys. Today **54**(5), 39 (2001).
[16] P.R. Hammar, B.R. Bennett, M.J. Yang, and M. Johnson, Phys. Rev. Lett. **83**, 203 (1999).
[17] C.M. Hu, J. Nitta, A. Jensen, J.B. Hansen, and H. Takayanagi, Phys. Rev. B **63**, 125333 (2001).
[18] H.J. Zhu, M. Ramsteiner, H. Kostial, M. Wassermeier, H.-P. Schönherr, and K.H. Ploog, Phys. Rev. Lett. **87**, 016601 (2001).
[19] A. Chrestin, T. Matsuyama, and U. Merkt, Phys. Rev. B **55**, 8457 (1997).
[20] G. Meier, M. Halverscheid, T. Matsuyama, and U. Merkt, J. Appl. Phys. **89**, 7469 (2001).
[21] A. Hubert and R. Schäfer, *Magnetic Domains—The Analysis of Magnetic Microstructures* (Springer, Berlin, 1998).
[22] Oommf, Object oriented micromagnetic framework, http://math.nist.org/oommf.
[23] MF3D, http://www.ramstock.de.
[24] T. Ando, A.B. Fowler, and F. Stern, Rev. Mod. Phys. **54**, 437 (1982).
[25] D.A. Baglee, D.K. Ferry, C.W. Wilmsen, and H.H. Wieder, J. Vac. Sci. Technol. **17**, 1032 (1980).
[26] E. Yamaguchi, Phys. Rev. B **32**, 5280 (1985).
[27] M. Johnson, B.R. Bennett, M.J. Yang, M.M. Miller, and B.V. Shanabrook, Appl. Phys. Lett. **71**, 974 (1997).
[28] G. Meier, D. Grundler, Ch. Heyn, and D. Heitmann, J. Magn. Magn. Mater. **210**, 138 (2000).
[29] U. Merkt, Phys. Rev. B **32**, 6699 (1985).
[30] D.J. Craik, *Magnetism—Principles and Applications* (Wiley, Chichester, 1995).
[31] R. Eiselt, M. Halverscheid, and G. Meier (unpublished).
[32] G. Bergmann, Phys. Rep. **107**, 1 (1984).
[33] D. Grundler, Phys. Rev. Lett. **86**, 1058 (2001).
[34] D. Grundler, Phys. Rev. B **63**, 161307 (2001).
[35] C.-M. Hu and T. Matsuyama, Phys. Rev. Lett. **87**, 066803 (2001).
[36] A. Bournel, P. Dollfus, P. Bruno, and P. Hesto, Eur. Phys. J. A **4**, 1 (1998).
[37] T. Matsuyama, C.-M. Hu, D. Grundler, G. Meier, and U. Merkt, Phys. Rev. B (to be published).
[38] G.E.W. Bauer, Phys. Rev. Lett. **69**, 1676 (1992).
[39] D.Y. Petrovykh, K.N. Altmann, H. Höchst, M. Laubscher, S. Maat, G.J. Mankey, and F.J. Himpsel, Appl. Phys. Lett. **73**, 3459 (1998).